Dispersion relation and optical transmittance of a hexagonal photonic crystal slab

T. Ochiai[1,2,*] and K. Sakoda[1]
[1]*Research Institute for Electronic Science, Hokkaido University, Sapporo 060-0812, Japan*
[2]*Research and Development Applying Advanced Computational Science and Technology, Japan Science and Technology Corporation, Tokyo 102-0081, Japan*
(Received 26 June 2000; revised manuscript received 31 October 2000; published 12 March 2001)

The dispersion relation and the optical transmittance of a two-dimensional photonic crystal composed of the hexagonal array of cylindrical air holes fabricated in a dielectric slab were analyzed by group theory and the numerical calculation based on the finite-difference time-domain method. The decay rate of the leaky modes that exist above the light line (the dispersion relation in air) in the band diagram was also evaluated, from which the absence of the coupling between certain internal eigenmodes and the external radiation field was shown. This phenomenon was related to symmetry mismatching by the group-theoretical argument. It was also shown that a certain leaky band has a quality factor as large as 3000 over its entire spectral range. These features as well as the opaque frequency regions due to symmetry mismatching were clearly demonstrated by the calculated optical transmission spectra.

DOI: 10.1103/PhysRevB.63.125107 PACS number(s): 42.70.Qs, 07.05.Tp, 41.20.Jb, 42.82.Et

I. INTRODUCTION

Recently, much attention has been paid to two-dimensional photonic crystals fabricated in dielectric slabs.[1–12] The radiation field in these crystals are controlled by the periodic dielectric structure in the two-dimensional plane and by the confinement due to the index difference in the third direction. Because the sophisticated techniques for the thin-film formation and lithography that are familiar in the fields of electronics and opto-electronics can be utilized for their fabrication, specimens of high quality and with large area are now available for experimental studies. The introduction of structural defects and waveguides in these crystals is also possible, and their various applications to opto-electronic devices have been proposed. Lasing with localized defect modes has already been reported.[12]

However, the confinement of the radiation field in the third direction is not complete. It is widely believed that only those modes that satisfy a certain relation between the eigenfrequency and the wave vector, which will be described later with the idea of the so-called *light line*, are confined and the rest of the eigenmodes have short lifetimes. This feature of the photonic crystal slabs may impose a serious constraint on their applicability, since the available frequency range is limited. On the other hand, to our knowledge, the consequence of the finite lifetime in the fundamental properties of the photonic crystal slabs such as the optical transmittance has not been fully clarified.

In this paper, we will report a theoretical investigation on the photonic band structure, the lifetime of the eigenmodes, and the optical transmittance of a two-dimensional hexagonal photonic crystal fabricated in a dielectric slab. The main features of the transmission spectra will be related to the spatial symmetry of the radiational eigenmodes and their lifetime. Especially, we will show the presence of the eigenmodes above the *light line* with extremely long lifetimes, which result in unexpectedly high transmittance. The symmetry of the eigenmodes was examined by both numerical calculation and the group-theoretical analysis. The amazing finding by Paddon and Young[13] that certain eigenmodes above the *light line* in a square lattice have infinite lifetimes was reproduced for our case, and its origin was clarified by the group theory. It will also be shown that the opaque frequency regions in the transmission spectra do not necessarily imply the presence of photonic band gaps.

II. SYMMETRY OF EIGENMODES

Figure 1 shows the schematic illustration of the two-dimensional photonic crystal slab that we deal with in this paper. It consists of the regular hexagonal array of air holes fabricated in a dielectric slab with the refractive index of 3.4 (GaAs). The right-hand side of the figure shows the top view of the configuration of several air holes. The lattice constant, the radius of the cylindrical holes, and the thickness of the slab are denoted by a, r, and d, respectively. We assume for the sake of simplicity that the structure is uniform in the z direction. We also assume that it is sandwiched by air. Photonic crystal slabs of this kind, which are referred to as the air-bridge type, have been one of the main subjects of the recent investigations. The following parameters were as-

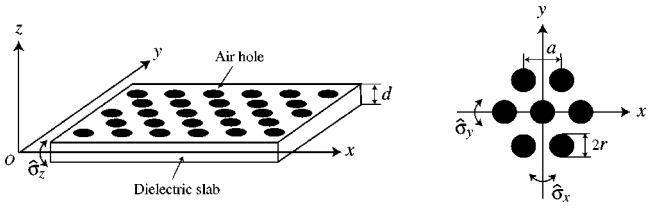

FIG. 1. Left: Schematic illustration of the two-dimensional photonic crystal slab. It is composed of a regular hexagonal array of cylindrical air holes fabricated in a dielectric slab. The structure is periodic and infinite in the x and y directions, and sandwiched by air in the z direction. The boundaries are located at $z=\pm d/2$. Right: Top view of the configuration of several air holes, where a and r denote the lattice constant and the radius of the air holes, respectively. For the numerical calculation, the following parameters were assumed: The refractive index of the dielectric slab = 3.4, $d=0.5a$, and $r=0.25a$.

sumed for the numerical calculation: $d=0.5a$ and $r=0.25a$. The structure has D_{6h} symmetry, which is the direct product of the C_{6v} and C_i point groups:

$$D_{6h}=C_{6v}\times C_i. \tag{1}$$

C_i consists of the identity operation $\hat{E}$ and the mirror reflection by the x-y plane, $\hat{\sigma}_z$. Thus any eigenmode of the radiation field should be symmetric ($\sigma_z=1$) or antisymmetric ($\sigma_z=-1$) about the x-y plane. In order to avoid unnecessary complexity, let us restrict our discussion to the symmetric modes in what follows. The antisymmetric modes can be treated in a similar manner.

Let us first examine what kind of radiational eigenmodes are expected to appear by the group-theoretical argument. The key idea is the reduction of the reducible representations given by the linear combination of unperturbed eigenfunctions. For the case of two-dimensional photonic crystals with infinite thickness[14] and general three-dimensional photonic crystals,[15,16] plane waves in free space were used as the unperturbed eigenfunctions. The group-theoretical prediction was usually satisfactory in the low-frequency range. For photonic crystals composed of dielectric spheres[17] and certain metallic systems,[18] the Mie resonance states may be used for this purpose. For the present problem, the guided modes in a uniform slab with a spatially averaged dielectric constant can be used as the unperturbed eigenfunctions.

In a uniform slab, the guided modes are classified into four categories according to the symmetry for the mirror reflection $\hat{\sigma}_z$ and to their polarizations. Those modes whose electric fields lie in the x-y plane are referred to as transverse electric (TE) modes, whereas those modes whose magnetic fields lie in the x-y plane are referred to as transverse magnetic (TM) modes. Each mode is also characterized by the wave number $k_\parallel$ in the x-y plane. The dispersion relations of the guided modes are obtained from the following equations:

$$\mu\kappa\cos\left(\frac{k_z d}{2}\right)-k_z\sin\left(\frac{k_z d}{2}\right)=0$$

$$\text{for TE modes with } \sigma_z=1, \tag{2}$$

$$\varepsilon\kappa\cos\left(\frac{k_z d}{2}\right)-k_z\sin\left(\frac{k_z d}{2}\right)=0$$

$$\text{for TM modes with } \sigma_z=-1, \tag{3}$$

$$\mu\kappa\sin\left(\frac{k_z d}{2}\right)+k_z\cos\left(\frac{k_z d}{2}\right)=0$$

$$\text{for TE modes with } \sigma_z=-1, \tag{4}$$

$$\varepsilon\kappa\sin\left(\frac{k_z d}{2}\right)+k_z\cos\left(\frac{k_z d}{2}\right)=0$$

$$\text{for TM modes with } \sigma_z=1, \tag{5}$$

where ε and μ denote the relative permittivity and permeability of the slab, respectively. In these equations, k_z is the z component of the wave vector defined in the dielectric slab,

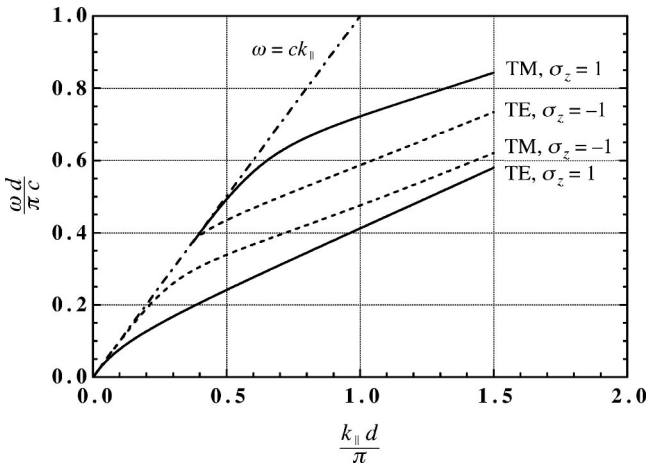

FIG. 2. The dispersion curves of the lowest four guided modes in a uniform slab with the refractive index of 2.86, which is the spatially averaged refractive index of the structure shown in Fig. 1. The ordinate is the normalized frequency, where d denotes the thickness of the dielectric slab. The abscissa denotes the normalized in-plane wave number. Solid lines represent the dispersion relations of modes with $\sigma_z=1$ whose in-plane components of the electric field are symmetric about the x-y plane, whereas broken lines represent those of modes with $\sigma_z=-1$ whose electric fields are antisymmetric. The dotted-broken line is referred to as the *light line*, which shows the dispersion relation in air.

whereas κ is the spatial decay constant in the z direction in the air region. When we denote the refractive index of the slab by n ($=\sqrt{\varepsilon\mu}$), k_z and κ are related to the angular frequency of the radiational eigenmode, ω, by

$$\omega^2=\frac{c^2}{n^2}(k_\parallel^2+k_z^2)=c^2(k_\parallel^2-\kappa^2), \quad \kappa>0 \tag{6}$$

where c is the light velocity in free space. The dispersion curves for the lowest four bands in the uniform slab with a refractive index of 2.86, which is the spatial average for the structure shown in Fig. 1, are depicted in Fig. 2, where two bands with $\sigma_z=-1$ are also shown for comparison. The ordinate and the abscissa denote the normalized frequency and the normalized wave number, respectively. In this figure, solid lines represent the dispersion relation for modes with $\sigma_z=1$, whereas broken lines represent that for modes with $\sigma_z=-1$. On the other hand, the dotted-broken line denotes the dispersion relation in air (free space), which we will refer to as the light line hereafter. If the eigenfrequency lies below the light line, the decay constant κ is real, and thus the eigenmode is confined in the slab. In other words, it is a guided mode. If the eigenfrequency lies above the light line, κ is purely imaginary, and the radiation field escapes from the slab. In this case, the radiational mode is not a real eigenmode, but is a resonant state with a complex ω, which is often called a leaky mode. Only the guided modes were plotted in Fig. 2.

One of the important features of the radiational bands in the uniform slab is that only the lowest two bands start from $\omega=0$, whereas higher bands have infrared cutoff frequen-

cies. For example, the third and fourth lowest bands, which are a TE mode with $\sigma_z=-1$ and a TM mode with $\sigma_z=1$, respectively, have a cutoff at

$$\omega_c=\frac{\pi c}{d\sqrt{n^2-1}}. \tag{7}$$

Therefore, when we deal with the low-frequency region as we will do in the following sections, it is fairly enough to take the lowest band into account. This treatment is especially justified for photonic crystals with small thickness, for which the cutoff frequencies are high. As we will see in the next section, the dispersion relation of modes with $\sigma_z=1$ can be actually well approximated for $\omega a/2\pi c\leqslant 0.5$ by the folding of the lowest dispersion curve into the two-dimensional Brillouin zone, provided that we take into consideration the mixing and the frequency splitting where more than one band with the same symmetry crosses each other. On the other hand, we have to take into account higher bands when we deal with higher-frequency regions. We should also note that the mixing of the TE and TM modes with the same σ_z takes place in the photonic crystal slabs.

Table I summarizes the results of the symmetry assignment by the folding of the dispersion curves of the lowest TE and TM modes into the first Brillouin zone. The irreducible representation of the electric field obtained by the reduction procedure mentioned previously are listed for three highly symmetric points, that is, the Γ, K, and M points. (For notation of the wave vectors, see Fig. 3.) These points are invariant by the symmetry operations that belong to the C_{6v}, C_{3v}, and C_{2v} point groups, respectively. Thus, their eigenmodes are classified according to the irreducible representations of the corresponding k groups,[19] which are listed in the fifth and sixth columns. In Table I, equivalent wave vectors with the same length in the extended-zone scheme, which are listed in the second column, are distinguished by a subscript. Their length and the number of the equivalent wave vectors are listed in the third and fourth columns.

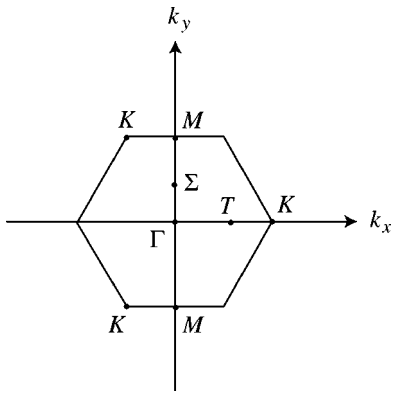

FIG. 3. The two-dimensional first Brillouin zone of the hexagonal lattice. There are two sets of three K points that are connected by reciprocal lattice vectors, and thus are equivalent to each other. One set among them are shown in this figure. The K point is invariant under symmetry operations of the C_{3v} point group. One of the three sets of two equivalent M points, which are invariant under symmetry operations of the C_{2v} point group, is also shown.

III. PHOTONIC BAND STRUCTURE AND TRANSMISSION SPECTRA

For the numerical calculation of the photonic band structure, we employed the method of the Fourier transformation of the time-correlation function of the electromagnetic field.[20] The temporal evolution of the electromagnetic field was calculated for each $\mathbf{k}_\parallel$ by the finite-difference time-domain (FDTD) method[21] with an initial condition that satisfied the Bloch theorem. Namely, we imposed the following conditions on the electric field $\mathbf{E}(\mathbf{r},t)$ and the magnetic field $\mathbf{H}(\mathbf{r},t)$:

$$\mathbf{E}(\mathbf{r}+\mathbf{a},0)=e^{i\mathbf{k}_\parallel\cdot\mathbf{a}}\mathbf{E}(\mathbf{r},0), \tag{8}$$

$$\mathbf{H}(\mathbf{r}+\mathbf{a},0)=e^{i\mathbf{k}_\parallel\cdot\mathbf{a}}\mathbf{H}(\mathbf{r},0), \tag{9}$$

TABLE I. The irreducible representations for the electric field of the guided modes in the uniform slab, whose wave vector, $k_\parallel$, is reduced in the two-dimensional first Brillouin zone of the hexagonal lattice that is shown in Fig. 3. The irreducible representations were calculated for the lowest TE mode with $\sigma_z=1$ and the lowest TM mode with $\sigma_z=-1$.

Symmetry	Wave vector	$\frac{k_\parallel d}{2\pi}$	Number of modes	TE mode with $\sigma_z=1$	TM mode with $\sigma_z=-1$
C_{6v}	Γ_0	0	1	Singular	Singular
	Γ_1	$2/\sqrt{3}$	6	$A_2+B_1+E_1+E_2$	$A_1+B_2+E_1+E_2$
	Γ_2	2	6	$A_2+B_2+E_1+E_2$	$A_1+B_1+E_1+E_2$
C_{3v}	K_0	2/3	3	A_2+E	A_1+E
	K_1	4/3	3	A_2+E	A_1+E
	K_2	$2\sqrt{7}/3$	6	A_1+A_2+2E	A_1+A_2+2E
C_{2v}	M_0	$1/\sqrt{3}$	2	A_2+B_1	A_1+B_2
	M_1	1	2	A_2+B_2	A_1+B_1
	M_2	$\sqrt{7/3}$	4	$A_1+A_2+B_1+B_2$	$A_1+A_2+B_1+B_2$

where **a** denotes the elementary lattice vector of the two-dimensional hexagonal structure. Boundary conditions of the same kind at arbitrary time t follow from these two conditions. In order to deal with the infinite extent of the air region, we imposed Mur's absorbing boundary condition of the first order[21] at $z=\pm(3/2)a$. The eigenfrequencies were obtained as the peak frequencies of the Fourier spectrum of the time-correlation function. Because of the mirror symmetry ($\sigma_z=1$) that we assumed in this paper and the boundary conditions, Eqs. (8) and (9), it was enough to treat only the upper half ($z\geqslant 0$) of a unit cell in the numerical calculation. When we deal with the Σ and T points, we could impose additional boundary conditions, which brought about both the reduction of the numerical task and the assignment of the spatial symmetry to each mode. For example, the Σ point is invariant by the mirror reflection $\hat{\sigma}_x$ that is illustrated in Fig. 1. So, its eigenmodes are classified into even ($\sigma_x=1$) and odd ($\sigma_x=-1$) modes. The former are also referred to as A modes, whereas the latter are referred to as B modes. Thus, we could reduce the spatial region for numerical calculation to the positive x region by imposing the symmetrical or antisymmetrical boundary condition. The same holds for the T point when we take into consideration the symmetry under the mirror reflection $\hat{\sigma}_y$ instead of $\hat{\sigma}_x$. As for the Γ point, both $\hat{\sigma}_x$ and $\hat{\sigma}_y$ operations could be used to distinguish two-dimensional as well as one-dimensional representations. The radiational modes that are attributed to a two-dimensional representation appeared as a degenerate pair of eigenmodes with complimentary symmetry properties. For instance, the eigenmodes with E_1 symmetry are characterized by $(\sigma_x,\sigma_y)=(-1,1)$ and $(1,-1)$. The unit cell was divided into 1152 meshes to discretize the Maxwell equations. The further decrease in the size of the spatial meshes did not give an apparent change in the eigenfrequencies.

The optical transmittance of ten lattice layers was calculated by the FDTD method with the lowest TE mode of a uniform slab with the refractive index of 3.4 as an incident wave. It was propagated in the Γ-K or Γ-M direction. The transmittance was evaluated by the ratio of the averaged Poynting vector of the transmitted wave to that of the incident wave.

The photonic band structures and the transmission spectra are shown in Fig. 4 for the Γ-K direction and Fig. 5 for the Γ-M direction. In the band diagrams, solid and open circles represent the odd (B) and even (A) modes, respectively. The light line is represented by a dotted-broken line. The symmetries of the eigenmodes obtained by the numerical calculation shown in these figures are consistent with the group-theoretical prediction that is given in Table I. They are also consistent, as they should be, with the compatibility relations[14,19] listed in Table II that relate the symmetries of modes with adjacent wave vectors. Such modes that do not match the group-theoretical prediction based on the folding of the lowest TE mode appeared at $\omega a/2\pi c\geqslant 0.57$.

It is known that the modes with $\sigma_z=1$ tend to have a photonic band gap below the light line. We can actually observe a band gap at $\omega a/2\pi c=0.26$–0.31. However, taking into account the leaky band that exists just above the light line in the same frequency region, this is not a true gap. This leaky band is of TM origin, and the corresponding unperturbed band with complex eigenfrequencies is obtained by the extrapolation of the dispersion curve shown in Fig. 2 beyond the infrared cutoff. As we also see in other frequency regions, one of the remarkable features of the band structure is the clear existence of the dispersion curves above the light line. These leaky bands have small decay rates around the Γ

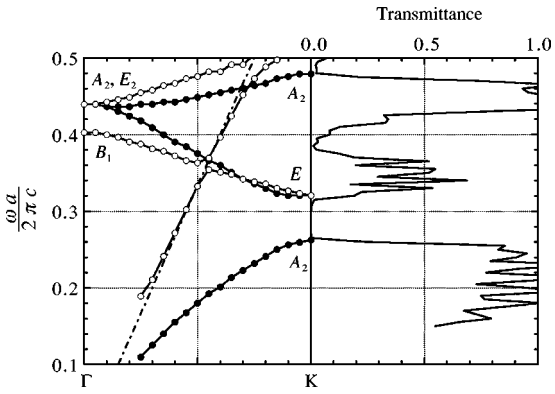

FIG. 4. The photonic band structure (left-hand side) and the optical transmittance (right-hand side) in the Γ-K direction. The ordinate is the normalized frequency, where a denotes the lattice constant. For numerical calculation, those parameters that are listed in the caption of Fig. 1 were used. In the band diagram, solid circles represent the odd (B) modes with $\sigma_y=-1$, whereas open circles represent the even (A) modes with $\sigma_y=1$. The irreducible representations of the k groups for the electric field are also shown for the Γ and K points. The transmittance was calculated for ten lattice layers with the lowest TE mode in the uniform slab with the refractive index of 3.4 as an incident wave. Thus, the incident wave has the symmetry of $\sigma_z=1$ and $\sigma_y=-1$. The even (A) modes do not contribute to the optical transmission, since they do not couple to the incident wave because of the symmetry mismatching.

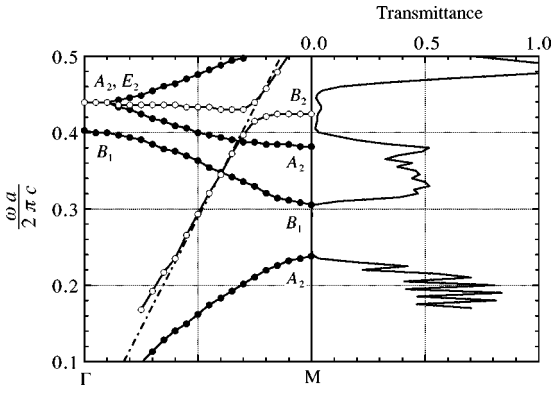

FIG. 5. The photonic band structure (left-hand side) and the optical transmittance (right-hand side) in the Γ-M direction. The same parameters as in Fig. 4 were assumed for numerical calculation. In the band diagram, solid circles represent the odd (B) modes with $\sigma_x=-1$, whereas open circles represent the even (A) modes with $\sigma_x=1$. The irreducible representations of the k groups for the electric field are also shown for the Γ and M points. The even (A) modes do not contribute to the optical transmission because of the symmetry mismatching.

TABLE II. The compatibility relations in the triangular lattice.

		T	Σ
Γ	A_1	A	A
	A_2	B	B
	B_1	A	B
	B_2	B	A
	E_1, E_2	$A+B$	$A+B$
K	A_1	A	-
	A_2	B	-
	E	$A+B$	-
M	A_1, B_1	-	A
	A_2, B_2	-	B

point, as we will see later. Especially, their decay rates are exactly equal to zero just at the Γ point.

Let us proceed to the transmission spectra. The lowest TE mode of the uniform slab, which was assumed for the incident wave, is odd about the $\hat{\sigma}_x$ or $\hat{\sigma}_y$ mirror reflection. Thus the even modes in the photonic crystal do not contribute to the optical transmission, since they do not couple to the incident wave because of the symmetry mismatching. This feature is clearly observed at $\omega a/2\pi c=0.26$–0.32 and 0.48–0.50 for the Γ-K direction, and $\omega a/2\pi c=0.24$–0.30 for the $\Gamma-M$ direction. In these frequency ranges, there is no odd mode and the transmittance is extremely small. The lowest transmittance is less than 10^{-3}. On the other hand, the transmittance is also small even when there is an odd mode if it is leaky. This is because the incident wave is diffracted into the air region, and the electromagnetic energy transmitted in the Γ-K or Γ-M direction becomes small. This feature is marked when the lifetime and/or the group velocity of the eigenmodes are small. The low transmittance of this kind is observed at $\omega a/2\pi c=0.38\sim0.41$ for the Γ-K direction and $\omega a/2\pi c=0.40\sim0.45$ for the $\Gamma-M$ direction. On the other hand, the transmittance is high when their lifetime is long. The high transmittance of this kind is observed around $\omega a/2\pi c=0.45$ for the Γ-K direction and around $\omega a/2\pi c=0.48$ for the Γ-M direction.

Let us conclude this section with the following. As was mentioned above, the transmittance may be low in two cases: (1) when there is no symmetry-matched mode and (2) when the lifetime of the eigenmode is short. It may also be low in the high-frequency region (3) when the Bragg diffraction in the x-y plane takes place. These facts imply that the frequency regions with low transmittance do not necessarily correspond to photonic band gaps. So, we must be careful when we compare the transmission spectra obtained by experimental observation and the band diagrams.

IV. DECAY RATES

As we saw in the previous section, the decay rate is an important quantity that characterizes the basic optical properties of the leaky modes. It can be evaluated by examining the temporal decay of the eigenmodes by the FDTD method.[22] For this purpose, we first excited the eigenmode by a dipole moment oscillating at its eigenfrequency located in the photonic crystal and observed its decay after switching off the oscillation. The accumulated electromagnetic energy $U(t)$ decreases with time as

$$U(t)=U(t_0)\exp\left[-\frac{\omega(t-t_0)}{Q}\right], \tag{10}$$

where t_0 stands for the switch-off time and Q is the quality factor of the eigenmode. In Fig. 6, the calculated Q^{-1} is plotted for the relevant bands. Solid and open circles represent the odd (B) and even (A) modes, respectively. Q^{-1} is equal to zero, or in other words, the lifetime is infinite near the K and M points, since the dispersion curves are located below the light line in these regions. A remarkable feature of this figure is that Q^{-1} is extremely small at the Γ point, where the modes shown in Fig. 6 have the B_1, A_2, and E_2 symmetries. As we shall see, this phenomenon originates from the symmetry mismatching between the guided modes in the photonic crystal and the diffracted radiational field in free space. Namely, the coupling between them is forbidden by symmetry, and the lifetime, and thus, Q are infinite.

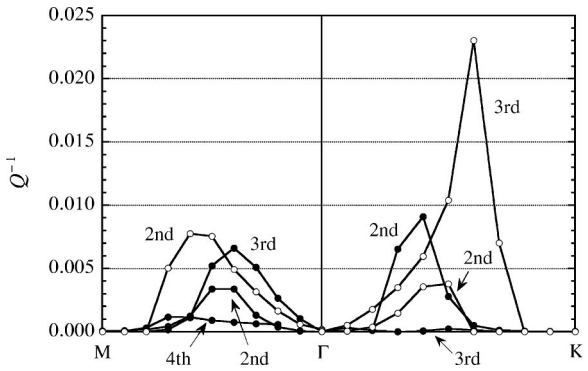

FIG. 6. The inverse of the quality factor (Q^{-1}) of several bands. Solid and open circles represent the odd (B) and even (A) modes, respectively. Q^{-1} is equal zero, or in other words, the lifetime is infinite near the K and M points, since the dispersion curves are located below the light line in those regions. A remarkable feature of this figure is that Q^{-1} is extremely small at the Γ point as well. This phenomenon originates from the symmetry mismatching between the guided modes in the photonic crystal and the diffracted radiation field in free space. Another important feature is that Q^{-1} is small for the third lowest odd mode in the Γ-K direction and for the fourth lowest odd mode in the Γ-M direction, which results in the high transmittance in the corresponding frequency regions. See text for details.

Let us examine the diffraction process of a mode with a wave vector $\mathbf{k}_\parallel$. Because of the conservation of the momentum in the x-y plane, the wave vector of a diffracted wave, $\mathbf{k}$, is generally given by

$$\mathbf{k}=\mathbf{k}_\parallel+\mathbf{G}_\parallel+k_z\mathbf{e}_z, \tag{11}$$

where $\mathbf{G}_\parallel$ and $\mathbf{e}_z$ are a reciprocal-lattice vector of the two-dimensional hexagonal structure and the unit vector in the z direction, respectively. k_z is given by

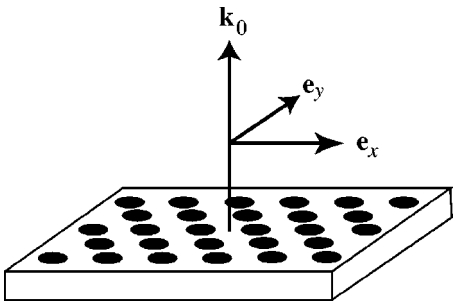

FIG. 7. Schematic illustration of the diffracted plane waves of the zeroth order for the Γ point. $\mathbf{k}_0$ denotes their wave vector. $\mathbf{e}_x$ and $\mathbf{e}_y$ denote their two independent polarizations. These two plane waves form the basis of the E_1 irreducible representation of the C_{6v} point group. See text for details.

$$k_z = \sqrt{\frac{\omega^2}{c^2} - |\mathbf{k}_\parallel + \mathbf{G}_\parallel|^2}. \tag{12}$$

It is easy to show that when $\omega a/2\pi c$ is less than $2/\sqrt{3}$, $\mathbf{G}_\parallel$ should be equal to zero for k_z to be real for the Γ point for which $\mathbf{k}_\parallel = \mathbf{0}$. Therefore, the diffracted waves are characterized by just one wave vector $\mathbf{k}_0$ given by

$$\mathbf{k}_0 = \frac{\omega}{c}\mathbf{e}_z . \tag{13}$$

We shall refer to these waves as the diffracted waves of the zeroth order. They have two polarization components as shown in Fig. 7, where $\mathbf{e}_x$ and $\mathbf{e}_y$ are the unit vectors in the x and y directions. These two waves, of course, have the same frequency. So, they are a degenerate pair of a two-dimensional irreducible representation of the C_{6v} point group. Their transformation by $\hat{\sigma}_x$ and $\hat{\sigma}_y$ is

$$(\sigma_x, \sigma_y) = (-1,1), \quad \mathbf{e}_x \tag{14}$$

$$(\sigma_x, \sigma_y) = (1,-1), \quad \mathbf{e}_y . \tag{15}$$

They are thus the basis set of the E_1 irreducible representation.[19] Because of the mismatching of the spatial symmetry, they can only couple to the E_1 modes in the hexagonal photonic crystal. This is the reason why the B_1, A_2, and E_2 modes at the Γ point shown in Fig. 6 do not couple to the radiation field in the air region and have the infinite quality factor. When the wave vector is near the Γ point, the coupling and Q^{-1} are still small although they are not exactly equal to zero. From this argument, it is expected that the E_1 modes at the Γ point should have short lifetimes. We found an E_1 mode at $\omega a/2\pi c = 0.54$ and its lifetime was really small.

A similar result was reported previously for a square lattice by Paddon and Young.[13] They found by numerical calculation that only the E mode at the Γ point was diffracted and had a finite lifetime. We can easily show by the similar argument as we did for the hexagonal lattice that the possible diffracted waves in the low-frequency region ($\omega a/2\pi c < 1$) has the E symmetry for the Γ point in the square lattice. Therefore, only the E modes in the photonic crystal couple to the external radiation field. The coupling for all other modes is forbidden by symmetry and they have infinite lifetimes. The absence of the coupling discussed here originates from the structural symmetry in the two-dimensional plane. So, it can also be observed in those specimens without the mirror symmetry about the x-y plane.

Another remarkable feature of Fig. 6 is the presence of leaky bands with very small decay rates. They are the third lowest odd band in the Γ-K direction and the fourth lowest odd band in the Γ-M direction. The quality factor of the former is greater than 3000 everywhere between the Γ and K points. The small decay rates of these two bands resulted in the high transmittance around $\omega a/2\pi c = 0.45$ in the Γ-K direction and around $\omega a/2\pi c = 0.48$ in the Γ-M direction.

Finally, let us give a qualitative estimation of the transmittance. The flow of the radiational energy is described by the group velocity v_g, which is given by the slope of the dispersion curve, if the dielectric constant of the photonic crystal is real.[23] When we denote the propagation length by L, the time necessary for the propagation is equal to L/v_g. The damping factor of the leaky mode is thus given by $\exp(-L\omega/Qv_g)$, to which the transmittance is proportional. As an example, let us examine the third lowest odd band in the Γ-K direction. Its group velocity is about $c/20$ at the middle of the band. If we assume that $L = 10a$, $Q = 3000$, and $\omega a/2\pi c = 0.45$, its damping factor is as large as 0.83. This is the origin of the high transmittance at this frequency. The third lowest odd mode may travel more than $50a$ in its lifetime. Within this length, the leaky mode may be regarded as a guided mode.

V. CONCLUSION

In summary, we have studied the dispersion relation of the radiational eigenmodes of a two-dimensional photonic crystal composed of the hexagonal array of cylindrical air holes fabricated in a dielectric slab by the group-theoretical argument and numerical calculation based on the FDTD method. The calculated dispersion relation was well approximated by the folding of the dispersion curve in a uniform slab with the spatially averaged refractive index into the two-dimensional Brillouin zone. The decay rate of the leaky modes that exist above the light line in the band diagram was also evaluated, from which the absence of the coupling between certain internal eigenmodes and the external radiation field was shown. This phenomenon was related to their symmetry mismatching by the group-theoretical argument. It was also shown that certain leaky modes have such large quality factors greater than 3000 that they behave as if they were guided modes over a distance larger than 50 times the lattice constant. All these features as well as the opaque frequency region due to the symmetry mismatching were clearly demonstrated by the optical transmission spectra calculated by the FDTD method.

ACKNOWLEDGMENTS

The authors are grateful to Mr. Takunori Ito for the numerical calculation of the dispersion curves of the uniform slab. This work was supported by ACT-JST (''Research and Development Applying Advanced Computational Science and Technology'' of Japan Science and Technology Corporation). K. S. was also supported by the Mitsubishi Foundation.

*Present address: Departamento de Física Teórica de la Materia Condensada, Facultad de Ciencias, Universidad Autónoma de Madrid, 28049 Madrid, Spain.

[1] J. D. Joannopoulos, R. D. Meade, and J. N. Winn, *Photonic Crystals* (Princeton University Press, Princeton, 1995).
[2] P. L. Gourley, J. R. Wendt, G. A. Vawter, T. M. Brennan, and B. E. Hammons, Appl. Phys. Lett. **64**, 687 (1994).
[3] M. Kanskar, P. Paddon, V. Pacradouni, R. Morin, A. Busch, J. F. Young, S. R. Johnson, J. Mackenzie, and T. Tiedje, Appl. Phys. Lett. **70**, 1438 (1997).
[4] S. Fan, P. R. Villeneuve, J. D. Joannopoulos, and E. F. Schubert, Phys. Rev. Lett. **78**, 3294 (1997).
[5] D. Labilloy, H. Benisty, C. Weisbuch, T. F. Krauss, R. M. De La Rue, V. Bardiral, R. Houdre, U. Oesterle, D. Cassagne, and C. Jouanin, Phys. Rev. Lett. **79**, 4147 (1997).
[6] B. D'Urso, O. Painter, J. O'Brien, T. Tombrello, A. Yariv, and A. Scherer, J. Opt. Soc. Am. B **15**, 1155 (1998).
[7] D. Labilloy, H. Benisty, C. Weisbuch, C. J. M. Smith, T. F. Krauss, R. Houdre, and U. Oesterle, Phys. Rev. B **59**, 1649 (1999).
[8] O. Painter, J. Vuckovic, and A. Scherer, J. Opt. Soc. Am. B **16**, 275 (1999).
[9] J. K. Hwang, H. Y. Ryu, and Y. H. Lee, Phys. Rev. B **60**, 4688 (1999).
[10] S. G. Johnson, S. Fan, P. R. Villeneuve, and J. D. Joannopoulos, Phys. Rev. B **60**, 5751 (1999).
[11] S. Kuchinsky, D. C. Allan, N. F. Borrelli, and J. C. Cotteverte, Opt. Commun. **175**, 147 (2000).
[12] O. Painter, R. K. Lee, A. Scherer, A. Yariv, J. D. O'Brien, P. D. Dapkus, and I. Kim, Science **284**, 1819 (1999).
[13] P. Paddon and J. F. Young, Phys. Rev. B **61**, 2090 (2000).
[14] K. Sakoda, Phys. Rev. B **52**, 7982 (1995).
[15] K. Ohtaka and Y. Tanabe, J. Phys. Soc. Jpn. **65**, 2670 (1996).
[16] K. Sakoda, Phys. Rev. B **55**, 15 345 (1997).
[17] K. Ohtaka (private communication).
[18] T. Ito and K. Sakoda (unpublished).
[19] See, for example, T. Inui, Y. Tanabe, and Y. Onodera, *Group Theory and Its Applications in Physics* (Springer, Berlin, 1990).
[20] C. T. Chan, Q. L. Yu, and K. M. Ho, Phys. Rev. B **51**, 16 635 (1995).
[21] A. Taflove, *Computational Electrodynamics* (Artech House, Boston, 1995).
[22] T. Ueta, K. Ohtaka, N. Kawai, and K. Sakoda, J. Appl. Phys. **84**, 6299 (1998).
[23] P. Yeh, J. Opt. Soc. Am. **69**, 742 (1979).